



PERGAMON

Scripta mater. 44 (2001) 953–958



www.elsevier.com/locate/scriptamat

STRAIN LOCALIZATION PATTERNS AT A CRACK TIP IN GENERALIZED SINGLE CRYSTAL PLASTICITY

Samuel Forest¹, Pascal Boubidi² and Rainer Sievert²

¹Ecole des Mines de Paris/CNRS, Centre des Matériaux/UMR 7633, BP 87 91003 Evry, France

²Bundesanstalt für Materialforschung und -prüfung, BAM V.23, Unter den Eichen 87, 12200 Berlin, Germany

(Received October 6, 2000)

(Accepted in revised form October 25, 2000)

Keywords: Crack; Single crystal; Crystal plasticity; Cosserat medium; Strain localization

Introduction

The asymptotic stress-strain field at a stationary crack tip in elastic-ideally plastic f.c.c. and b.c.c. single crystals, as determined by Rice *et al.* [1], turns out to be locally constant within angular sectors. It involves shear displacement discontinuities at sector boundaries, that can be interpreted as strain localization bands. The numerical analysis of the same problem using finite strain crystal elastoplasticity in [2] reveals that the condition of constant stress state in each sector must be relieved because of possible local unloading, but also that the strain localization patterns pertain. Discrete models based on dislocation dynamics also lead to strongly localized dislocation distributions near the crack tip and to the progressive formation of the predicted sectors [3]. Experimental observations in a b.c.c. single crystal in [4] confirms the existence of such intense deformation bands radiating from the crack tip.

The fact that the strong strain gradients developing in the vicinity of the crack tip may affect the local mechanical response of a crystalline solid suggests that generalized continuum theories, including Cosserat, strain gradient and non local models, could be helpful for computing more realistic local stress-strain fields. The strain gradient model used in [5] results in a substantial increase of the tractions ahead of the tip of a mode I crack within a domain of characteristic size related to the constitutive intrinsic length. This monitoring of the local strain field enables one to improve the prediction of subsequent crack growth. The use of a generalized continuum model also strongly affects the localized deformation modes as demonstrated in [6] in the case of single crystals. In particular, classical crystal plasticity theory predicts two types of deformation bands in single crystals undergoing single slip: slip bands lying in the slip plane of the locally activated slip system, or kink bands lying in a plane normal to the slip direction of the slip system [7]. The formation of a kink band is associated with the development of strong lattice rotation gradients at its boundary and may therefore be precluded if the model incorporates additional hardening due to lattice curvature [6]. The present work investigates the effect of a generalized continuum theory on the localized deformation patterns arising at the crack tip in elastoplastic f.c.c. single crystals. Important consequences are expected regarding crack branching after stable crack growth.

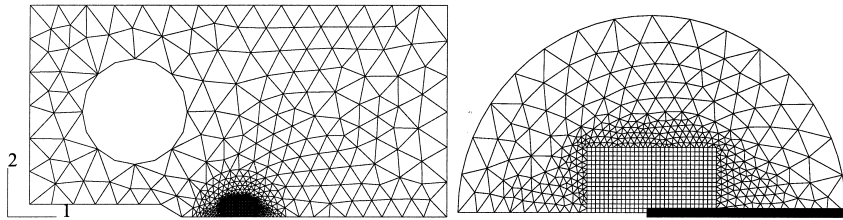


Figure 1. Finite element mesh of CT specimen (left, the mesh of the pin is not represented); mesh of the crack tip zone, the nodes belonging to the ligament being represented by black squares (right).

Presentation of the Calculations

The finite element mesh of the considered single crystalline CT specimen to be computed under plane strain conditions is represented on Figure 1. A regular mesh with quadratic elements and reduced integration is used at the crack tip. Such a mesh has been shown in [7] to be able to capture shear bands of any orientation and thus to minimize the mesh-dependence of the results associated with localization phenomena. It is important since the orientation of the localization bands must be a prediction of the model. Displacement in direction 2 is prescribed to the pin whereas the ligament is fixed in this direction. An additional boundary condition needed for the generalized continuum to be presented, is vanishing lattice rotation at the ligament for symmetry reasons. The Cosserat single crystal plasticity model used in the following is motivated and described in details in [6,8] and the main constitutive equations are briefly recalled within the small deformation and rotation framework. The degrees of freedom of the theory are the displacement u_i and the lattice rotation vector ϕ_i . The corresponding deformation and curvature tensors e_{ij} and κ_{ij} are split into elastic and plastic parts according to:

$$e_{ij} = u_{i,j} + \epsilon_{ijk}\phi_k = e_{ij}^e + e_{ij}^p, \quad k_{ij} = \phi_{i,j} = k_{ij}^e + k_{ij}^p \quad (1)$$

$$\dot{e}_{ij}^p = \sum_{s=1}^n \dot{\gamma}^s m_i^s n_j^s, \quad \dot{k}_{ij}^p = \sum_{s=1}^n \frac{\dot{\theta}^s}{l_p} \xi_i^s m_j^s \quad (2)$$

The amount of slip, the slip direction and the normal to the slip plane of slip system s are denoted by $\dot{\gamma}^s, m_i^s$ and n_i^s and ξ_i^s is the vector product of n^s and m^s . θ_i^s represents the local curvature angle over a characteristic size l_p and is accommodated here only by edge-type dislocations. However the whole Cosserat effect lies in the very simple hardening rule:

$$\tau_c^s = \tau_0 + H |\theta^s| \quad (3)$$

where τ_c is the critical resolved shear stress for plastic activation, τ_0 its initial value for perfectly plastic crystals, and H the additional hardening modulus associated with lattice curvature. A Schmid law is used for the activation of the slip systems with a viscoplastic formulation to avoid possible indeterminacy [2]. More elaborate constitutive equations than (3) can be proposed but this one contains the main effect to be investigated. The material parameters concern single crystal nickel-base superalloy SC16 at 650°C [9]. In particular, $\tau_0 = 500\text{MPa}$. Octahedral slip only is taken into account for simplicity, involving 12 $\{111\}\langle 110\rangle$ slip systems. Parameter H will be varied from 0 to 10000MPa to investigate the lattice curvature effect on localization. In practice, there are 3 ways to identify parameter H for a specific material. In [6] it is suggested that the characteristic size associated with some strain localization modes, on the one hand, and, on the other hand, direct identification from dislocation dynamics simulations of flexion tests followed by tension can be used. It will appear here that H could

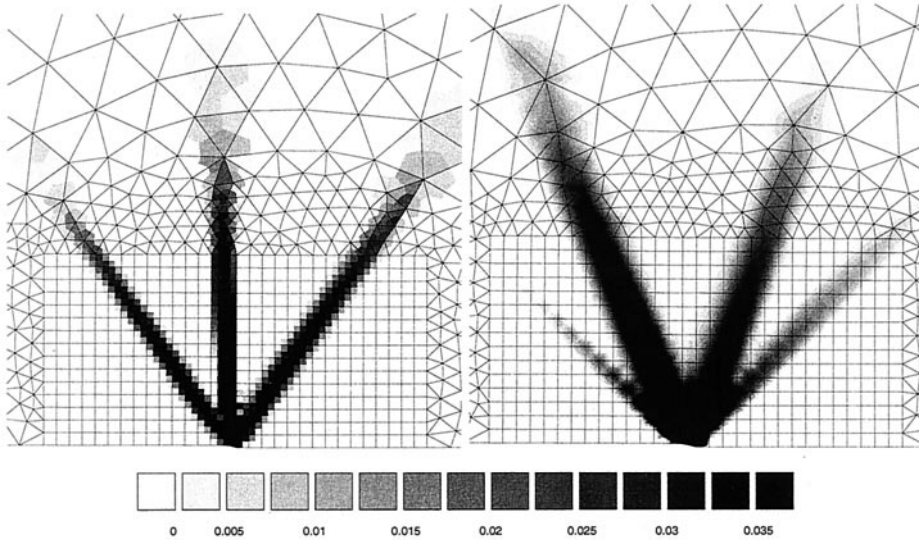


Figure 2. Strain localization pattern at the crack tip: (011)[100] crack (left) and (001)[100] crack (right), equivalent plastic strain.

also be adjusted to recover the experimental crack growth rate (see also [5]). The orientation of the specimen will be described by, firstly, the crack plane and, secondly, the initial crack growth direction.

Results

The structure of the localization band patterns found at the tip of (011)[100] and (001)[100] cracks are described by Figures 2 and 3 for a computation with vanishing H . In this case, the results are almost identical with that obtained with a classical finite strain crystal plasticity model. Three main types of bands are found. In the band (2) of the (011)[100] crack (see Figure 3 for the band numbers), two slip systems are activated simultaneously with the same amount of slip and result in an effective macroscopic (100)[011] slip band. Similarly, the second band can be interpreted as a kink band for the effective slip

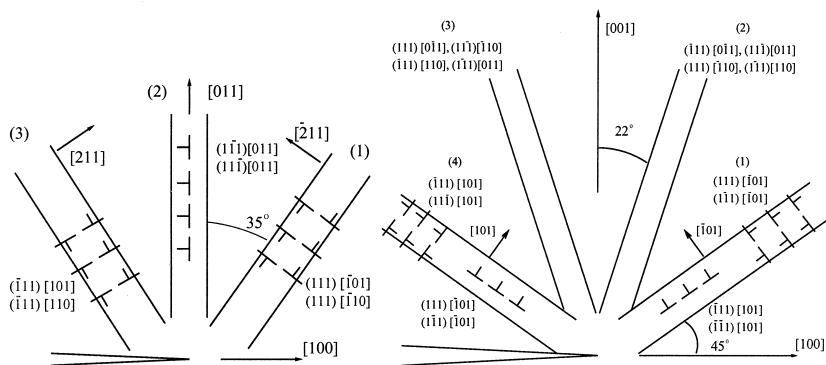


Figure 3. Localization band patterns: (011)[100] crack (left) and (001)[100] crack (right); the indicated slip systems are significantly activated in the nearest band.

TABLE 1

List and Structure of Investigated Localization Bands for Several Crack Configurations For the cases illustrated in Figure 3, the band orientations and types are listed in the order given by the numbers on Figure 3, i.e. counterclockwise starting from the right; the bands in brackets do not appear for sufficiently high values of H

crack orientation	number of bands classical (Cosserat)	band characteristics (orientation and type)
(011)[100]	3 (1)	(55° <i>kink</i>), 90° <i>slip</i> , (125° <i>kink</i>)
(001)[110]	3 (2)	55° <i>slip</i> , (90° <i>kink</i>), 125° <i>slip</i>
(001)[100]	4 (2)	(45° <i>slip+kink</i>), 68° <i>multislip</i> , 112° <i>multislip</i> , (135° <i>kink+slip</i>)
(011)[011]	3 (2)	68° <i>multislip</i> , (90° <i>slip+kink</i>), 112° <i>multislip</i>

system (111) $\bar{2}$ 11]. The kink band is associated with significant localized lattice rotation and therefore strong lattice curvature. In contrast slip bands like (2) induce almost no lattice rotation at all. The pattern observed at the (001)[100] crack tip is much more complicated and four slip systems are activated simultaneously in each band. In band (1), the amount of slip is the same for the four systems and the band can be interpreted as the superposition of an effective $\bar{1}$ 01[101] slip band and of an effective (101) $\bar{1}$ 01] kink band. In band (2), the activated slip systems can be divided into two groups of two slip systems with different amount of slip for each group. We will call it a multislip band. This results apparently in a non-crystallographic localization plane. Similar non-crystallographic shear bands for double slip have been obtained in [7]. Note that all four bands are associated with strong lattice rotations. A summary of all investigated orientations is given in Table 1.

If sufficiently strong additional hardening H is introduced, the picture is drastically changed, as shown on Figure 4. For the (011)[100] crack, the two kink bands have disappeared, as it could have been expected from the bifurcation analysis of [6]. Note that for the dual orientation (001)[110] the vertical kink band disappears and two inclined slip bands remain. In the (001)[100] case, two multislip bands only remain. Lattice curvature inside these bands leads to higher local stresses and therefore more

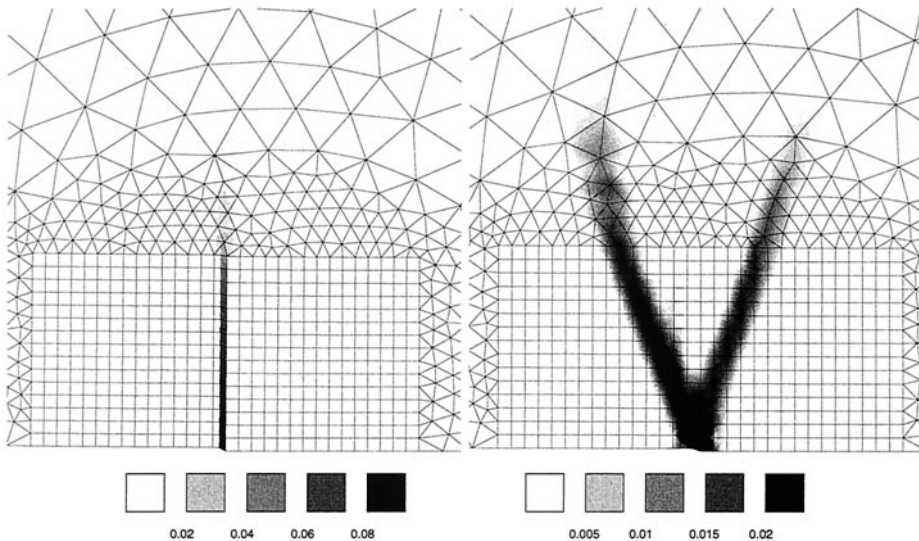


Figure 4. Strain localization patterns at the crack tip including lattice curvature effects: (011)[100] crack (left) and (001)[100] crack (right); contour of plastic strain.

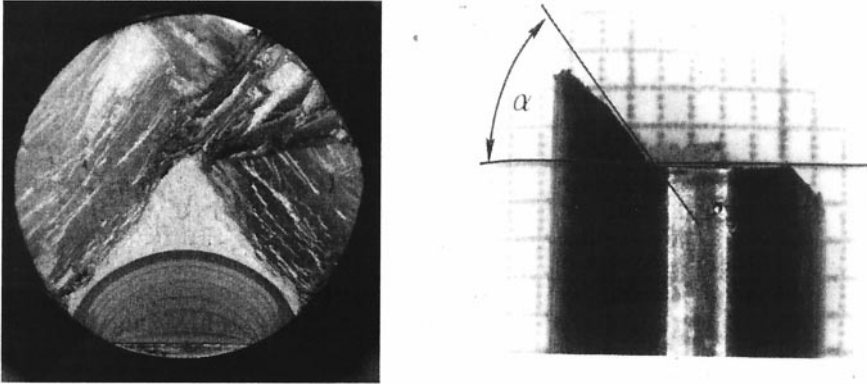


Figure 5. Final unstable crack path for two sharply notched [001] SC16 specimens after cyclic loading (specimen diameter: 9mm): fracture surface for a (001)[100] initial crack (left, the tensile direction [001] is normal to the fracture surface) and side view of the fracture surface for a (001)[110] initial crack showing the trace of the bifurcation plane (111) (right) [9].

limited localization. It must be noted that contrary to the isotropic elastoplastic case, the localization patterns computed under plane stress conditions are not significantly different. The introduction of moderate work-hardening leads to more diffuse deformation but does not significantly alter the structure of the crack tip stress-strain field.

Conclusions and Prospects

The previous computations indicate that, if additional hardening due to lattice curvature is introduced in continuum modelling, (effective) kink bands are precluded at the crack tip in favour of (effective) slip bands. If all possible bands are associated with lattice curvature, some of them can subsist. The physical relevance of the result is difficult to assess since only scarce precise observations of the crack tip in single crystals are available. In [4], a b.c.c. single crystal is carefully studied for crack orientation that is similar to our (001)[110] crack for symmetry reasons. Indeed the vertical kink band expected in the classical analysis does not seem to be present. However no special attention is paid to this point in [4]. If localization bands are regarded as privileged bifurcation paths for possible crack branching, the present work leads us to postulate the following: Crack branching from a stable path to a kink plane is not possible and, more generally, crack deviation to a localization band with strong lattice curvature is limited. This is supported by some experimental results provided in [9] and in Figure 5 for two sharply notched SC16 specimens under cyclic loading. The initial sharp notches respectively correspond to (001)[100] and (001)[110] cracks. After a certain number of cycles, crack growth becomes unstable: in the first case, the fracture surface is complex but the crack remains globally in its initial plane whereas, in the second case, it deviates on a (111) plane, as expected from Table 1 ((001)[110] crack). A decisive experiment would be to consider a (011)[100] specimen for which we expect no crack deviation in spite of the kink bands predicted by the classical crystal plasticity. Furthermore more realistic fully three-dimensional crack configurations must be investigated numerically.

Acknowledgment

The authors are grateful for the financial support of the Deutsche Forschungsgemeinschaft (DFG) for a project on the “Modelling of the hardening behavior under strong inhomogeneous deformation for the calculation of large cracks” (OL 50/7-1).

References

1. J. R. Rice, D. E. Hawk, and R. J. Asaro, *Int. J. Fract.* 42, 301 (1990).
2. A. M. Cuitino and M. Ortiz, *Modelling Simul. Mater. Sci. Eng.* 1, 225 (1993).
3. H. H. M. Cleveringa, E. van der Giessen, and A. Needleman, in *Proceedings of the 20th Riso International Symposium on Materials Science*, p. 293, Riso National Laboratory, Roskilde, Denmark (1999).
4. T. W. Shield and K.-S. Kim, *J. Mech. Phys. Solids.* 42, 845 (1994).
5. Z. C. Xia and J. W. Hutchinson, *J. Mech. Phys. Solids.* 44, 1621 (1996).
6. S. Forest, *Acta Mater.* 46, 3265 (1998).
7. S. Forest and G. Cailletaud, *Eur. J. Mechan. A/Solids.* 14, 747 (1995).
8. S. Forest, F. Barbe, and G. Cailletaud, *Int. J. Solids Struct.* 37, 7105 (2000).
9. J. Ziebs and H. Frenz, in *Schaufeln und Scheiben in Gasturbinen-Werkstoff und Bauteilverhalten*, Sfb 339, TU Berlin, pp. D1IV-1 (1997).